Improved Dissolution of an Enteric Polymer and its Amorphous Solid Dispersions by Polymer Salt Formation

Qingqing Qi[1], Lynne S. Taylor[1]

[1]Department of Industrial and Physical Pharmacy, College of Pharmacy, Purdue University, West Lafayette, Indiana 47907, United States

Graphical Abstract

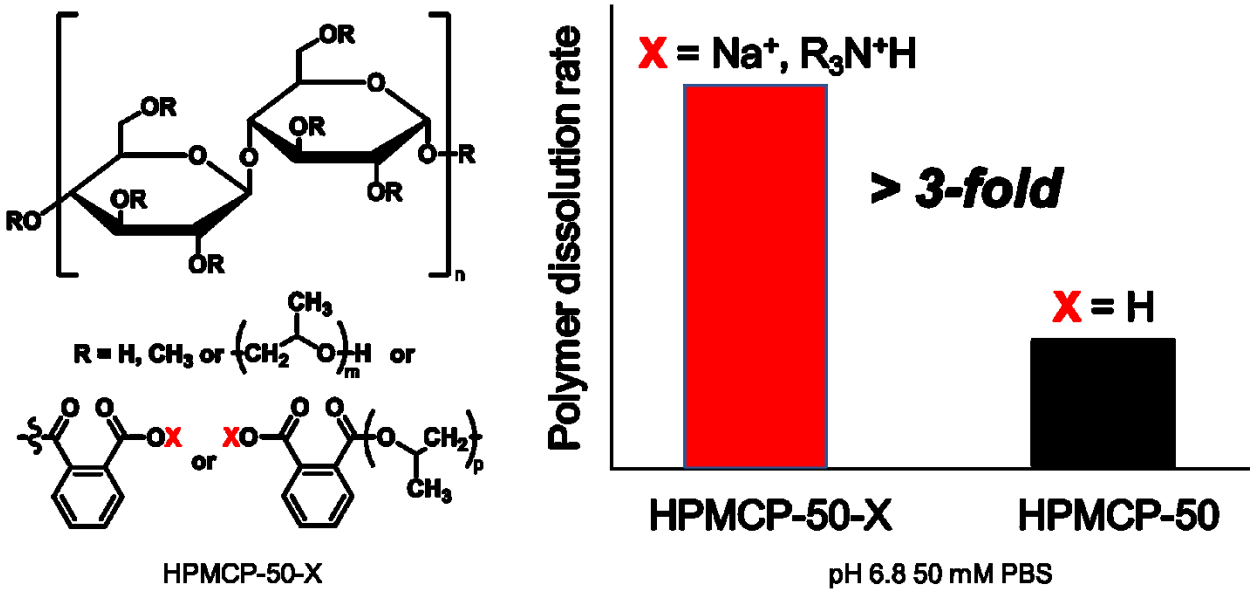

Abstract

Weakly acidic polymers, historically used as enteric coatings, are increasingly being employed in solubility-enhancing amorphous solid dispersion (ASD) formulations. However, there is a lack of fundamental understanding around how these carboxylic acid-containing polymers dissolve, in particular when molecularly mixed with a lipophilic drug, as in an ASD. Identification of critical factors dominating their dissolution is vital for rational design of new polymers with enhanced release properties to address contemporary ASD delivery challenges, notably achieving good release at higher drug loadings. Herein, after identification of polymer solubilization via ionization as the rate limiting step for dissolution, hydroxypropylmethyl cellulose phthalate (HP-50) was converted to a salt by neutralization of the phthalic acid groups with different bases. Surface

normalized dissolution was performed to assess the dissolution rate improvement achieved by polymer pre-ionization via salt formation. Polymer salts showed ~3-fold faster release than HP-50 at pH 6.8 (50 mM sodium phosphate buffer, PBS). Importantly, a polymer salt was able to maintain a rapid dissolution rate, irrespective of the buffer capacity of the medium, whereas the protonated polymer showed greatly diminished dissolution as medium buffer capacity decreased toward physiological gastrointestinal tract values. HP-50 and two polymer salts were formulated into ASDs with miconazole, a lipophilic and weakly basic antifungal drug, at a 20% drug loading. Rapid drug release rates were achieved with polymer salt ASDs, whereby drug release was 14 times faster than from the protonated HP-50 ASD. This study highlights the critical role of polymer ionization and buffer capacity in the dissolution of HP-50-based systems and how pre-ionization via polymer salt formation is a successful strategy for the design of new polymers for improved ASD performance.

Keywords. Polymer salt; release performance; enteric polymer dissolution, amorphous solid dispersion, pre-ionization

1. INTRODUCTION

Enteric polymers have been used historically as tablet coatings to delay drug release until after the formulation has exited the stomach. Ideally, the enteric coating dissolves rapidly when the pH of the gastrointestinal milieu reaches the threshold pH where the polymer becomes soluble. However, several *in vivo* investigations have shown a lag time for disintegration of enteric coated tablets in the small intestine.[1-3] In contrast, during *in vitro* testing in 50 mM pH 6.8 phosphate buffer, coating disintegration is typically rapid.[1, 2] This discrepancy is thought to be due, at least in part, to the low buffer capacity of intestinal fluids, whereby there is a lower pH at the polymer-water surface, reducing the rate of polymer dissolution.[4] Harianawala et al. experimentally demonstrated a lower pH close to the surface of a dissolving enteric polymer film, in agreement with theoretical models.[4, 5] More recently, polymers originally developed for use as enteric coatings, including hydroxypropylmethyl cellulose acetate succinate (HPMCAS) and hydroxypropylmethyl cellulose phthalate (HPMCP), have been used in the formulation of amorphous solid dispersions (ASD).[6] When used for ASD applications, the drug is molecularly dispersed in the polymer matrix. Thus, in contrast to enteric coatings, some drug may be released

from the ASD formulation at the low pH conditions of the gastric compartment, followed by rapid polymer dissolution and release of the remaining drug in simulated intestinal fluid.[7, 8] ASDs based on enteric polymers therefore require the pH in the intestine to exceed a certain value for complete release of the drug. While media buffer capacity is known to be an important factor impacting the disintegration time of enteric coated tablets, the impact of this parameter on the dissolution of ASDs prepared with enteric polymers has not been widely studied. ASDs of a drug and enteric polymer are fundamentally different from enteric coatings in that the drug is blended with the polymer in the ASD formulation, whereby the molecular level mixing of drug and polymer can impact the polymer dissolution process, and *vice versa*.[9] Furthermore, polymer dissolution, rather than rupture of a polymer coating, is required for the drug to be released from the ASD. Therefore, polymer dissolution is an important process for ASDs and requires more in-depth consideration.

Polymer dissolution is complex and involves the following steps 1) ingress of water into the polymer matrix, 2) disentanglement of polymer chains, 3) release of polymer at the surface and diffusion across the aqueous boundary layer.[10] For enteric polymers, an ionization step is also necessary.[11] Ionization of the polymer chains leads to additional polymer hydration, solubilizing the polymer chains. Polymer hydration increases the molecular mobility of the polymer chain, enabling reptative disentanglement followed by diffusion into the bulk medium. The rate limiting steps for the dissolution of weakly acidic polymers are not well understood and somewhat controversial.[10, 12, 13] With their increasing use in ASD formulations, this is a critical gap that needs to be addressed, in particular for scenarios where addition of the drug alters the polymer dissolution rate.

Reiser pioneered a model based on percolation theory to describe acidic polymer dissolution predicated on the formation of an intermediate gel layer. He concluded that movement of solvent species from one ionizing site on the polymer backbone to another in the gel layer was the rate limiting step, that a critical number of ionized sites per polymer molecule are necessary for dissolution to commence, and that the rate of dissolution is subsequently dependent on the number of ionized sites in excess of this critical concentration.[13] Willson developed a different model more akin to models developed for small molecule dissolution, whereby he considered that polymer detachment occurred only from the outer surface layer (i.e. no gel layer), where the

dissolution rate was related to the extent of ionization of a given polymer chain.[12] Both of these models worked well to describe the dissolution of acid polymers of low molecular weight which do not have entangled chains. Nguyen and Fogler developed a model for a higher molecular weight enteric polymer where the important factors were considered to be buffer species concentration and pK_a relative to the surface and bulk pH, as well as hydrodynamic factors and polymer chain disentanglement kinetics.[11] In recent studies from our group, we noted that different drugs modify enteric polymer dissolution rate to different extents depending on the specific drug studied.[9, 14, 15]

The goal of this study was to better understand factors impacting the dissolution of enteric polymers used in ASD formulations. HPMCP was selected as a model ionizable amphiphilic cellulose derivative. The surface normalized dissolution rate of HPMCP in different media was investigated, varying the buffer species cation size, pK_a and concentration. Next, polymer salts formed via acid-base reaction were generated to evaluate the impact of pre-ionization and counterion type on polymer dissolution kinetics. Finally, drug release from ASDs prepared with the protonated HPMCP polymer versus the polymer salt was compared, using miconazole as a model poorly soluble lipophilic drug.

2. MATERIALS

Miconazole, taurine (TAU), triethylamine and N, N-diisopropylethylamine (DIPEA) were purchased from Fisher Chemicals (Fair Lawn, NJ, USA). Hydroxypropylmethyl cellulose phthalate (HPMCP-50, HP-50) was supplied by Shin-Etsu Chemical Co. (Tokyo, Japan). Hexafluoroisopropanol (HFIP), BIS-TRIS, tris base (THAM), 2-amino-2-methyl-1-propanol (AMP), morpholine, BIS-TRIS propane, sodium methoxide (0.5 M in methanol) and tetrabutylammonium hydroxide (1.0 M in methanol) were from Sigma-Aldrich (St. Louis, MO, USA) respectively. Phosphate buffer (50 mM, pH 6.8) was prepared by dissolving 6.96 g of sodium phosphate dibasic anhydrous and 7.04 g of sodium phosphate monobasic monohydrate in 2 L of deionized water. Both sodium phosphate dibasic and sodium phosphate monobasic monohydrate were purchased from Macron Fine Chemicals (Philipsburg, NJ, USA). The deuterated DMSO for nuclear magnetic resonance (NMR) spectroscopy was purchased from Fisher Chemicals (Fair Lawn, NJ, USA). Deuterated chloroform and deuterium oxide were from Cambridge Isotope Laboratories (Tewksbury, MA, USA).

3. METHODS

3.1. Ionized Polymer Preparation

HPMCP-50-Na (HP-50-Na) was prepared from HP-50 by addition of sodium base (Figure S1-3) and HP-50-tetrabutylammonium (PTBA) was prepared by salt metathesis reaction and characterized as described in Figure S4.

Preparation of polymer salts with amines is summarized below. Briefly, the amine (1.61 mmol, 1.0 equiv to the phthalic acid in 1.0 g of HP-50) was added into a clear solution of 1.0 g HP-50 dissolved in MeOH/DCM (10:90 v/v) under stirring at room temperature. The mixture was stirred for 30-60 min, followed by solvent removal using rotary evaporation at 40 ^{o}C using a Heidolph Hei-VAP Core rotary evaporator (Heidolph Instruments, Schwabach, Germany) coupled to a Ecodyst EcoChyll S cooler (Ecodyst, Apex, NC, USA) under reduced pressure. Additional MeOH was used in the case of tris base due to its lower solubility in DCM.

3.2. Preparation of Amorphous Solid Dispersions (ASDs) of Miconazole

ASDs were prepared by solvent evaporation at 50 °C using a Heidolph Hei-VAP Core rotary evaporator (Heidolph Instruments, Schwabach, Germany) coupled to an Ecodyst EcoChyllS cooler (Ecodyst, Apex, NC, USA) under reduced pressure. DCM/MeOH (50:50 v/v) was used to dissolve polymer and miconazole. The dissolved mixture was stirred for 30 min at room temperature followed by solvent evaporation. The obtained ASDs were pulverized with a 6750 Freezer/Mill cryogenic impact mill (SPEX SamplePrep, Metuchen, NJ, USA) after a secondary drying step in a high vacuum oven for 48 h at room temperature. The pulverized ASD powder was stored in a desiccator over calcium sulfate at room temperature overnight and used without further treatment.

HP-50-TEA (PTEA) ASD can also be made in a one-pot procedure. Triethylamine (1.0 equiv to the phthalic acid in HP-50) was added into a solution of HP-50 in MeOH/DCM (10:90 v/v) under stirring. After 60 min, miconazole was added and stirred for another 30 min before the solvent was evaporated.

3.3. Water Uptake Studies

HP-50 and HP-50-Na were pulverized and dried at 50 $^{\circ}$C in an oil bath in the presence of P_2O_5 under vacuum for 24 h. 200 mg of neat polymer powder was placed in a 4 mL glass vial and the

powder was leveled. The open vial was then stored at 100% RH at 37 °C. The water sorption of neat polymers was measured gravimetrically at various time intervals for up to 96 hours.

3.4. Determination of the Glass Transition Temperature (T_g)

Differential Scanning Calorimetry (DSC)

The neat polymers and ASD powders prepared by solvent evaporation were loaded into standard aluminum pans sealed with an aluminum lid. The glass transition temperatures were analyzed by a Q2000 differential scanning calorimeter with a refrigerated cooling accessory (TA Instrument, New Castle, DE, USA). The sample was equilibrated at -30 °C and then heated from -30 to 140 °C at 5 °C/min with a modulation of ±0.796 °C every 60 s and then cooled to -30 °C at 10 °C/min. A second heating step was performed, heating to 140 °C at 10 °C/min. The heating and cooling cycle was repeated twice, and the second cycle was used for analysis. The temperature accuracy of the Q2000 was validated by running a 5 °C/min heating ramp on a sample of indium. During the experiment, a nitrogen flow of 50 mL/min was maintained to create a dry environment.

Dynamic Mechanical Analysis (DMA)

Dynamic mechanical analysis (DMA) was performed using a Discovery DMA 850 from TA Instruments (New Castle, DE, USA) for neat polymers and ASDs. Approximately 50–100 mg of the powder sample was spread uniformly onto a compression clamp fixture. The powder was then heated at rate of 2 ºC/min with an applied frequency of 1 Hz and a strain level of 0.1%. The peak of the tan δ curve plotted *versus* temperature was taken as the T_g. Sample testing was performed in triplicate.

3.5. Nuclear Magnetic Resonance (NMR) Spectroscopy

^{1}H NMR, ^{19}F NMR, and ^{13}C NMR spectroscopy were performed using a Bruker DRX 500 MHz spectrometer (Billerica, MA, USA). The spectrum of the as-received miconazole was comparable to literature reports according to ^{1}H NMR and ^{13}C NMR spectra in deuterated chloroform.[16]

3.6. Fourier Transform Infrared (FTIR) Spectroscopy

Thin films of neat HP-50-Na and HP-50 were prepared by spin-coating for collection of transmission IR spectra. The polymer was dissolved in MeOH/DCM (2:1 v/v) at a concentration of 50 mg/mL for spin-coating. 100 µL of solution was deposited onto a thallium bromoiodide (KRS-5) window (Harrick Scientific Corporation, Ossining, NY, USA), then the substrate was first spun for 15 s at 50 rpm and then for another 50 s at 2500 rpm using a spin coater (Chemat Technology Inc., Northridge, CA, USA). The spin-coating process was conducted in a humidity-controlled glovebox and then the substrate was dried in vacuum oven at room temperature for 24 h. The IR spectra were collected in transmission mode using a Bruker Vertex 70 FTIR spectrometer (Billerica, MA, USA). 64 scans were collected for both the background and samples at a resolution of 4 cm^{-1}. The data were analyzed using OPUS software (version 7.2, Bruker, Billerica, MA, USA).

3.7. Elemental Analysis of HP-50-Na

Elemental analysis was undertaken at Galbraith Laboratories, Inc (Knoxville, TN, USA). HP-50-Na powder was dried at 80 ºC under vacuum for 10 h before analysis. Carbon and hydrogen were determined using the PerkinElmer 2400 Series II CHNS/O Analyzer (Waltham, MA, USA). 1.0-5.0 mg was placed in a tin capsule and burnt in pure oxygen at 920-980 °C under static conditions to produce combustion products of CO_2 and H_2O. The PE-2400 automatically separates and analyzes these products in a self-integrating, steady state thermal conductivity analyzer. Acetanilide was used for calibration. The quantitation limit was 0.5% for each of the two elements. For oxygen determination, a Thermo Finnigan FlashEA™ 1112 Elemental Analyzer ((Bedford Heights, OH, USA) was used. 1.0-4.0 mg sample was placed in a silver weighing capsule which was crimped and then introduced into the combustion furnace. The FlashEA 1112 pyrolyzes the sample in an inert atmosphere (helium). During pyrolysis, nitrogen, hydrogen, and carbon monoxide are formed when they contact the nickel-plated carbon catalyst at 1060 °C. The pyrolysis products cross an adsorption filter where the carbon monoxide and hydrogen are separated via a chromatographic column. The FlashEA 1112 then automatically analyzes the carbon monoxide in a self-integrating, steady state thermal conductivity analyzer, and provides the oxygen percentage as a weight percent based on manual weight entry. Benzoic acid was used for calibration. For sodium determination, an ICP-OES Optima 3300DV (PerkinElmer, Waltham, MA, USA) was used to measure the characteristic emission spectrum by optical spectrometry. Approximately 100

mg of sample was digested. The digestion solution was nebulized and the resulting aerosol was transported to the plasma torch. Element-specific emission spectra were produced by radio-frequency inductively coupled plasma. The spectra were dispersed by a grating spectrometer, and the intensities of the emission lines were monitored by a photosensitive device.

3.8. Thermogravimetric Analysis (TGA) Profile of HP-50-Na

Thermal stability of HP-Na was assessed using a Discovery TGA 5500 (TA Instruments, New Castle, DE, USA) under a nitrogen purge. The sample was heated at 10°C/min from ambient conditions to 500°C. Degradation assessment was performed in the TRIOS software using the tangent intersection method and weight loss methods. Weight loss experienced prior to 140°C was attributed to water/solvent loss.

3.9. Dissolution of Polymers and Amorphous Solid Dispersions Using a Rotating Disk Apparatus

Surface area normalized dissolution was carried out using an intrinsic dissolution rate measurement assembly (Agilent, Santa Clara, CA, USA). The neat polymer was used as is, while ASDs were pulverized. 100 mg of material was compressed at a pressure of 1500 psi with a hydraulic press (Carver Inc., Wabash, IN, USA) in a circular intrinsic die of diameter 8 mm (corresponding to a surface area of 0.5 cm^2), and the compression pressure was held for one minute. The die was then attached to a paddle rotating at 100 rpm unless otherwise stated. All dissolution experiments were performed in 100 mL of pH 6.8 phosphate buffer (50 mM) at 37 °C unless otherwise specified.

3.10. Concentration Analysis of Drug and Polymer

For the release studies, 0.2 mL and 0.03-0.2 mL of the dissolution medium were withdrawn for miconazole and polymer concentration analysis respectively and replaced with fresh buffer to maintain the volume at 100 mL. The typical time points taken were 10, 20, 30, 40, 50, 60, 80, 100 and 120 min. For miconazole, 0.2 mL of the sample was diluted by the addition of 0.4 mL of deionized water and 0.6 mL of methanol to obtain a clear solution, and the drug concentration was analyzed using a high-performance liquid chromatography (HPLC) system (1260 Infinity, Agilent, Santa Clara, CA, USA). For the HPLC analyses, a mobile phase of 80% (v/v) methanol in

deionized water and 0.05% TFA (v/v) at a flow rate of 0.7 mL/min at 40 °C with an injection volume of 8 µL and an ultraviolet (UV) detection wavelength of 210 nm were used. The separation column used was an Ascentis Express C18 (Sigma-Aldrich, St. Louis, MO, USA) with dimensions of 10 cm × 3.0 mm, 2.7 µm particle size. Polymer quantification was carried out with colorimetric measurement.[17] 10 µL of phenol solution (4 g in 1 mL deionized water) was added to 0.4 mL of sample diluted to contain less than 100 µg/mL HP-50 and vortexed for 5 seconds. Then 1 mL of sulfuric acid was added and left to react for 60 min.

4. RESULTS

4.1. Impact of Buffer Species on the Intrinsic Dissolution Rate of HPMCP

Previous studies have demonstrated that the size of the base cation can impact the dissolution rate of acidic polymers.[18] Herein, to evaluate the impact of buffer cation size on the dissolution rate of the protonated polymer, phosphate buffers with different counterions were used, at an equivalent molarity, and hence buffer capacity. The size of the cation ranged from Na with a Van der Waals radius of 227 pm to Cs with a radius of 343 pm for the alkali metals, as well as two organic cations, ammonium and tetrabutyl ammonium which have Van der Waals volumes of 25.28 $Å^3$ and 300.36 $Å^3$ respectively, which correspond to radii of 182 and 415 pm respectively assuming spherical geometry. The hydrated radius of the cations is similar for K, Cs and ammonium, and Na has the largest value (Table S1). Figure 1 summarizes the dissolution data of HPMCP in the various buffers. Release is linear as a function of time, and approximately 25-35% release is achieved within 60 min. It is apparent from Figure 1 that cation size, for the range of sizes tested, has little impact on the polymer dissolution rate, with the exception of tetrabutyl ammonium, where the dissolution rate is slightly slower. Given the weak correlation between counterion size and dissolution rate, an extended set of buffers was used for evaluation of polymer dissolution rate in order to elucidate the impact of other factors.

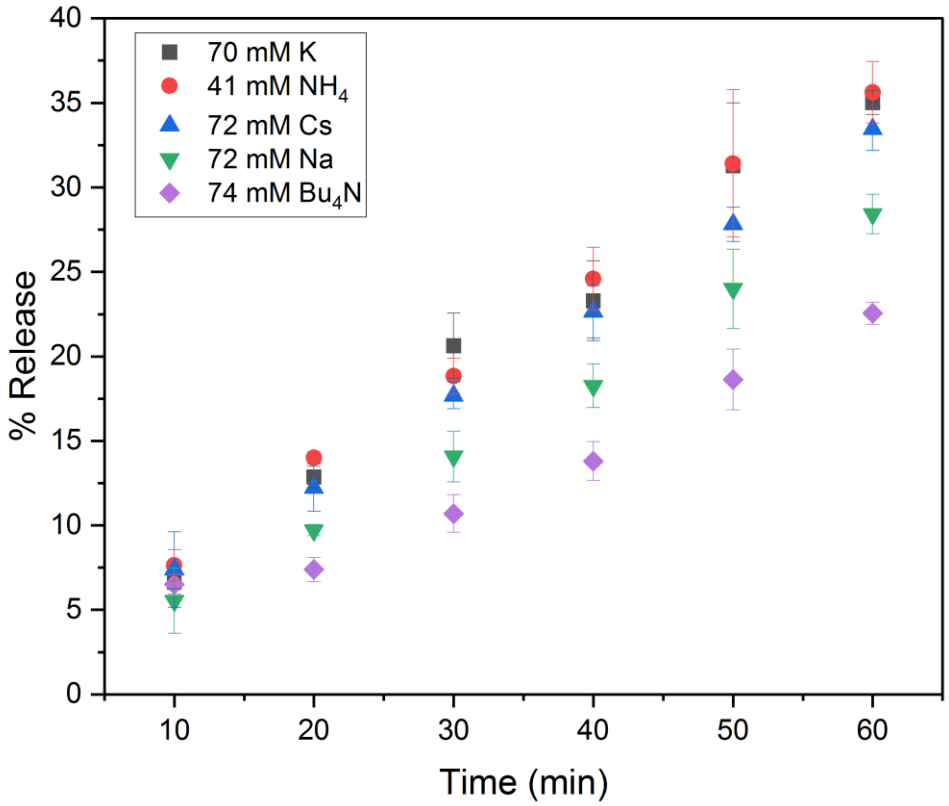

Figure 1. Release profiles of HP-50 in pH 6.8 50 mM phosphate buffer with different cations. Error bars indicate standard deviation, n = 3.

Dissolution of HP-50 with additional buffers at pH 6.8 was performed and compared with the corresponding dissolution profile in 50 mM sodium phosphate buffer. The composition of each buffer is shown in Table S2 and selected polymer release profiles are shown in Figure 2. Release data for additional buffer systems can be found in the supporting information (Table S2, Figure S7).

From Figure 2, it is apparent that the polymer dissolution rate is highly dependent on the buffer species present, with the bis tris buffer providing the fastest polymer dissolution rate, and TEA the slowest rate. There is clearly no correlation between cation size and polymer dissolution rate. Other pertinent properties that appear to trend with the polymer release rate are the buffer species pK_a and buffer capacity at the dissolution pH. The buffer systems which show poor polymer release have higher pK_a values (Table 1) and consequently lower buffer capacities at pH 6.8. In contrast, buffers where more rapid polymer dissolution is observed, have higher buffer capacities and pK_a values close to the dissolution pH.

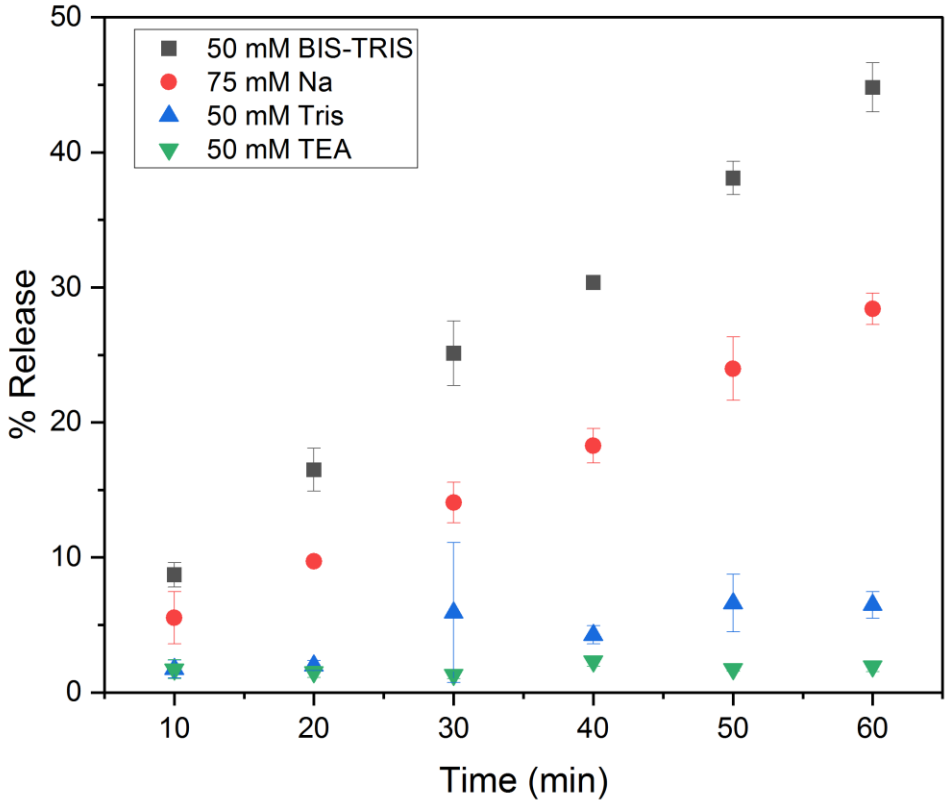

Figure 2. Release profiles of HP-50 in pH 6.8 hydrochloric acid-amine buffers using 75 mM sodium, 50 mM phosphate buffer as reference (red). Error bars indicate standard deviation, n = 3.

4.2. Polymer Salts

Since HPMCP is a weak acid, it is possible to make polymer salts by reaction with bases. The structure of HPMCP-50-X (HP-50-X), where X is a cationic counterion, is shown in Figure 3. The counterions used to prepare polymer salts are listed in Table 1, together with properties of interest. Formation of a polymer salt was verified using NMR spectroscopy, with results presented in the supplemental information (Figure S9).

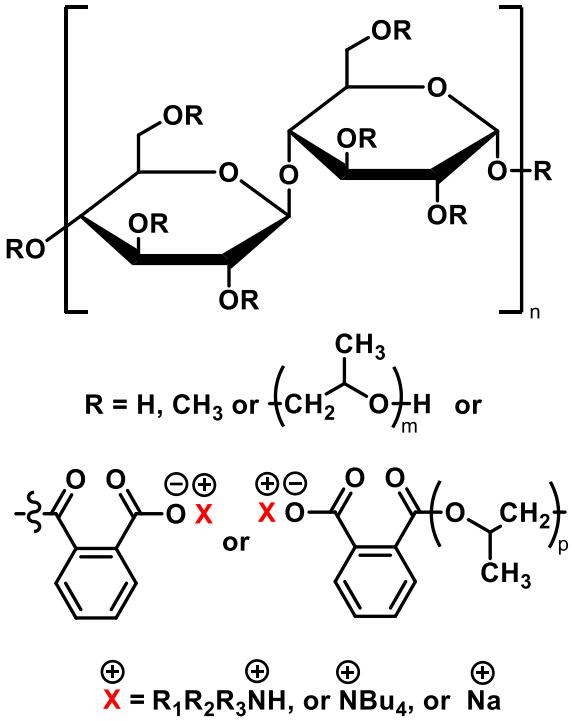

Figure 3. HPMCP-50-X (HP-50-X) salts where X is the cationic counterion with select examples of the counterion shown.

Table 1. Summary of counterions explored for polymer salt formation.

Polymer code (cation precursor)	Structure of precursor	pK_a	MW (g/mol)	logP	Amine type[a]	# OH groups	# N atoms	VdW volume (Å^3)[b]
PAMP (AMP)[c]	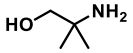	9.7	89.1	-0.6	1°	1	1	100
PTHAM (Tris base)	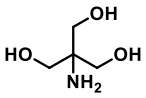	8.1	121.1	-2.7	1°	3	1	117
PMP (Morpholine)		8.5	87.1	-0.4	2°	1	1	90
PBTP (BIS-TRIS propane)	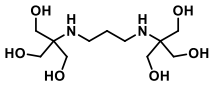	9.0, 6.8	282.3	-4.7	2°	6	2	276

PDIP (DIPEA)	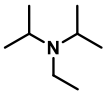	10.8	129.3	2.1	3°	0	1	161
PBTM (BIS-TRIS)	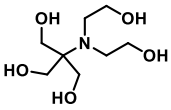	6.5	209.2	-3.3	3°	5	1	204
PTEA (Triethylamine)	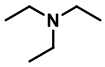	10.2	101.2	1.3	3°	0	1	127
PTBA (Tetrabutylammonium)	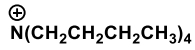		242.5			0	1	300
HP-Na (Sodium ion)	Na^+		23.0			0	0	49

[a] 1°: primary amine, 2°: secondary amine, 3° tertiary amine; [b]Van der Waals volumes are calculations using Chemicalize (ChemAxon); [c]AMP is the abbreviation for 2-Amino-2-methyl-1-propanol; [d] DIPEA is the abbreviation for N,N-Diisopropylethylamine;

4.3. Polymer Characterization

Sodium and Ammonium Content in HP-50-X

HP-50-Na was characterized by ^{1}H NMR spectroscopy (Figure S2) and elemental analysis. Sodium constitutes 3.38%-3.52% by weight corresponding to a molar content of sodium ranging from 91-95% indicating nearly complete ionization. Ammonium content was measured to be around 100% by ^{1}H NMR in deuterated solvent as illustrated in Figure S4.

Fourier Transform Infrared (FTIR) Spectroscopy of HP-50-Na

Infrared spectroscopy confirmed the appearance of new bands characteristic of the carboxylate ion (1600 cm^{-1}) as shown in Figure 4, consistent with polymer ionization.

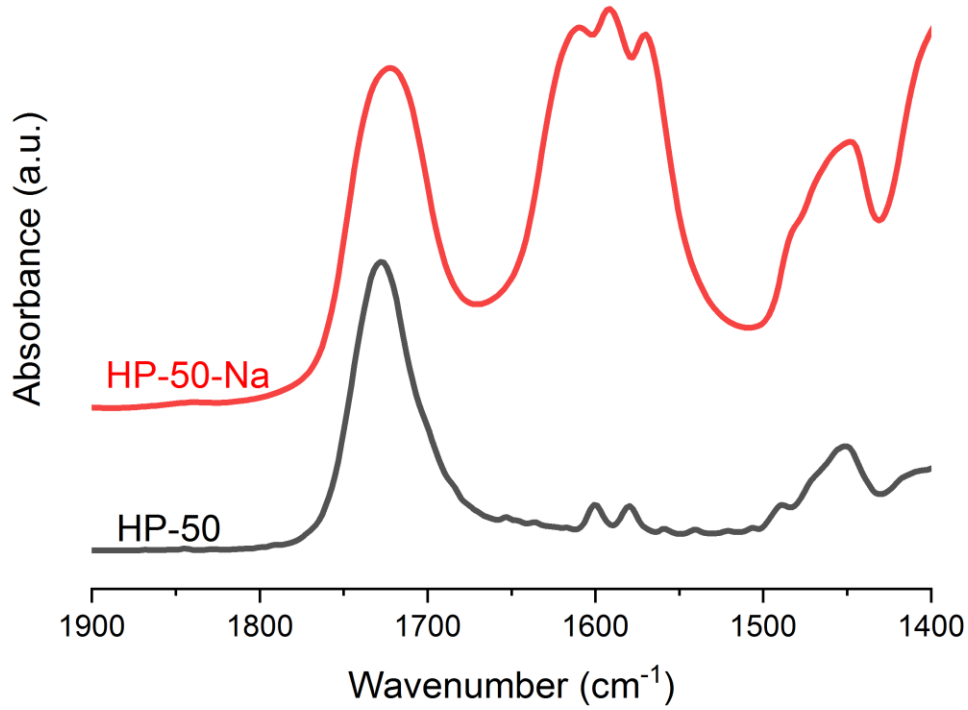

Figure 4. FTIR spectra of the carbonyl region of HP-50-Na versus HP-50.

Thermogravimetric analysis (TGA) of HP-50-Na

The thermal stability of HP-50-Na was assessed by nonisothermal thermogravimetric analysis. Based on the tangent intersection analysis, three temperatures correspond to degradation events of the polymer: 174.2 °C (corresponding to 0.47% total weight loss), 267.7 °C (corresponding to 6.8% total weight loss), and 327.2 °C (corresponding to 26.8% total weight loss) (Figure S10).

4.4. Glass Transition Temperature (T_g) by DSC and DMA

T_g values were measured by either DSC or DMA with results summarized in Table 2. T_g was noted to vary from a low of 55°C for the tris polymer salt to a high of 231°C for the sodium salt.

Table 2. Summary of glass transition temperature of neat polymers and ASDs

Neat polymer	PAMP	PTHAM	PMP	PBTP	PDIP
DSC onset T_g (ºC)	68.2 (1.9)	54.9 (1.7)	58.1 (1.4)	84.5 (0.9)	78.1 (1.8)
Neat polymer	PBTM	PTEA	PTBA	HP-50	HP-Na
DSC onset T_g (ºC)	-[a]	84.0 (1.7)	92.1 (2.1)	127.1 (2.7)	-[a]

DMA peak T_g (°C)[c]	135.7 (2.1)	-[b]	-[b]	172.8 (0.4)	231.3 (2.8)
ASD polymer (20% DL)	HP-50	HP-Na	PTEA		
DSC onset T_g (°C)	83.4 (0.4)	-[a]	77.2 (0.9)		
DMA peak T_g (°C)	142.0 (2.0)	216.2 (0.6)	116.7 (1.1)		

[a]Not detected. [b]Not determined. [c]Peak of *tan δ* was used.

Standard deviations are shown in parentheses, where n = 3.

4.5. Release Profiles of Ionized Polymers

Surface normalized dissolution of the sodium polymer salt was performed to compare the release improvement after pre-ionization (Figure 5). HP-50-Na showed ~3-fold faster dissolution than the protonated polymer as shown in Figure 5. Close to 100% of the Na-polymer dissolved at 80 min, while only ~40% of the protonated polymer was released over the same time period. To probe the impact of the cation on the polymer dissolution process, a series of amine polymer salts was synthesized. Polymers with an ammonium cation showed nearly complete dissolution after 80 min, with no notable difference observed among the different cations (Figure 6), regardless of amine molecular weight or lipophilicity (Table 1), whereby a similar dissolution rate to the Na salt was observed.

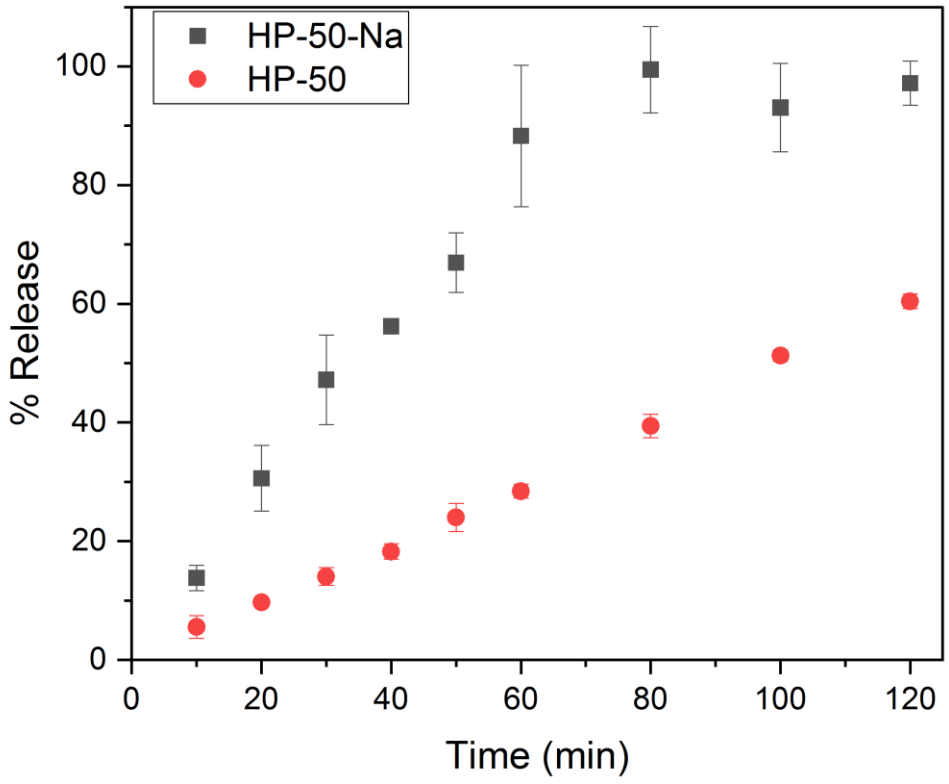

Figure 5. Release profiles of HP-50-Na and HP-50. Error bars indicate standard deviation, n = 3.

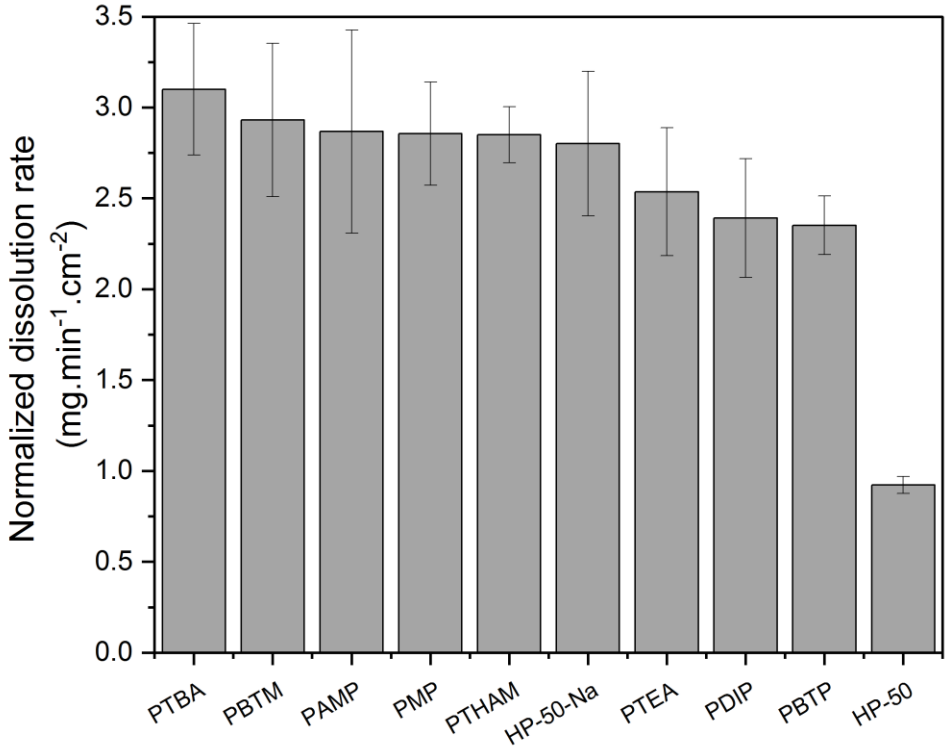

Figure 6. Normalized dissolution rate of pre-ionized and protonated polymers. Error bars indicate standard deviation, n = 3.

4.6. Hydration of Neat Polymers

The water sorption of select polymers was measured gravimetrically at various time intervals for up to 96 hours with results summarized in Figure 7. The Na polymer salt absorbed the most water, reaching more than 40% water. The protonated polymer had a much lower water content, while the three amine salts had intermediate water contents, with the salt with the more hydrophilic BIS-TRIS cation absorbing more water than the salts with more lipophilic cations, DIPEA and tetrabutylammonium salts, although the differences were smaller than might be anticipated from the chemical structure of the cations.

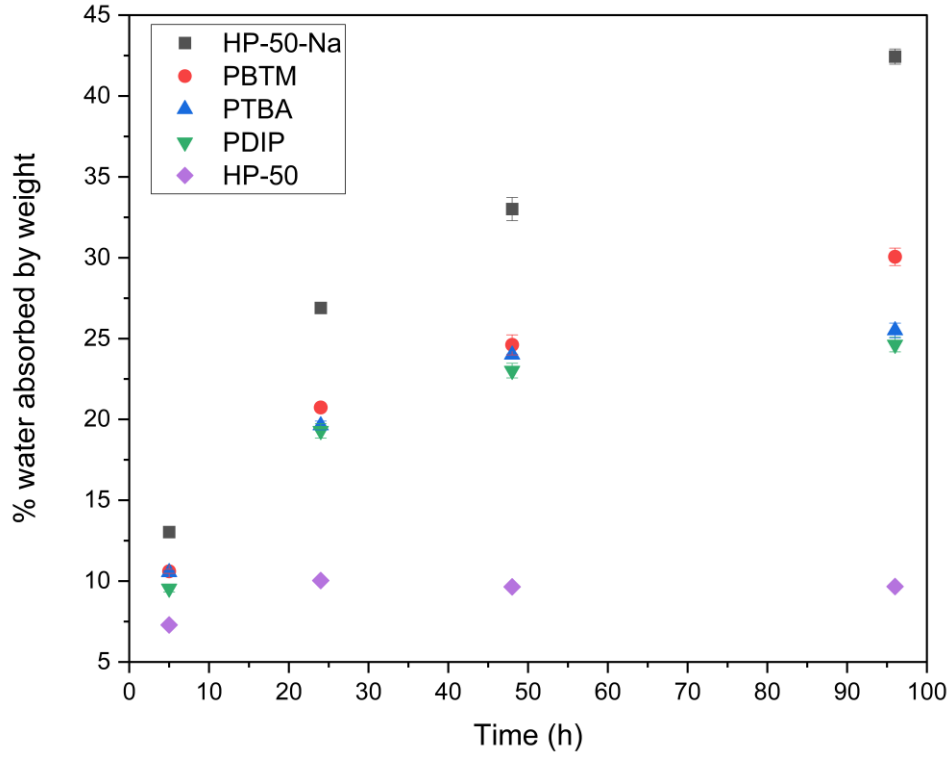

Figure 7. Hydration of pre-ionized polymers and HP-50 during storage at 100% RH. Error bars indicate standard deviation, n = 3.

4.7. Buffer Capacity Impact on Polymer Salt Dissolution

It is well known that the dissolution rate of enteric polymers depends on the buffer capacity of the medium.[19] To evaluate if salt formation leads to a polymer that is more robust to buffer capacity variations, the dissolution rate of the protonated polymer and the sodium polymer were compared in two solutions with different buffer capacity. As is apparent from Figure 8, the dissolution rate of HP-50-Na is the same in both solutions, while the protonated polymer shows a 6-fold reduction in dissolution rate upon changing from 50 to 5 mM phosphate buffer, corresponding to a buffer capacity of 29 and 3 $mM \cdot \Delta pH^{-1}$, respectively.

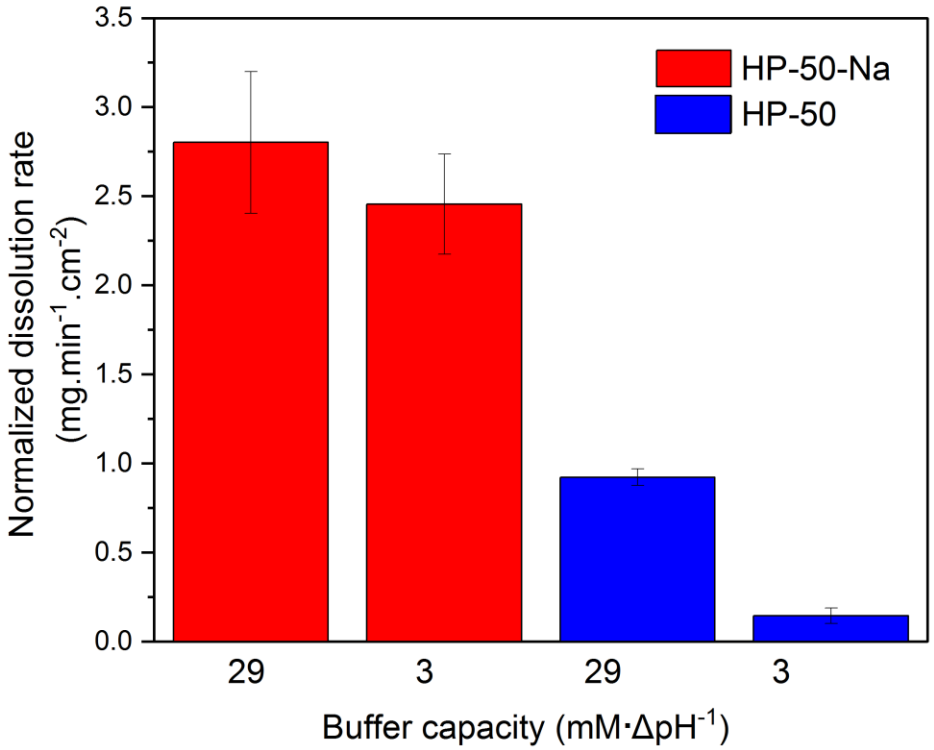

Figure 8. Normalized polymer release rate of HP-50-Na and HP-50 in solutions of different buffer capacities. Error bars indicate standard deviation, n = 3.

4.8. Effect of Ionization Percentage on Dissolution Rate of Neat Polymers (HP-50-BIS-TRIS)

To further probe the relationship between polymer ionization and dissolution, a series of partially neutralized polymer salts was prepared by reaction with BIS-TRIS. Normalized dissolution rates are summarized in Figure 9 where the dissolution of the protonated polymer in a BIS-TRIS phosphate buffer is shown for comparison. It is apparent that the dissolution rate decreases as the percent ionization is reduced from 100 to 20% ionized. The largest decrease in dissolution rate occurs when the extent of ionization is reduced from 100 to 80% with a more modest decline thereafter.

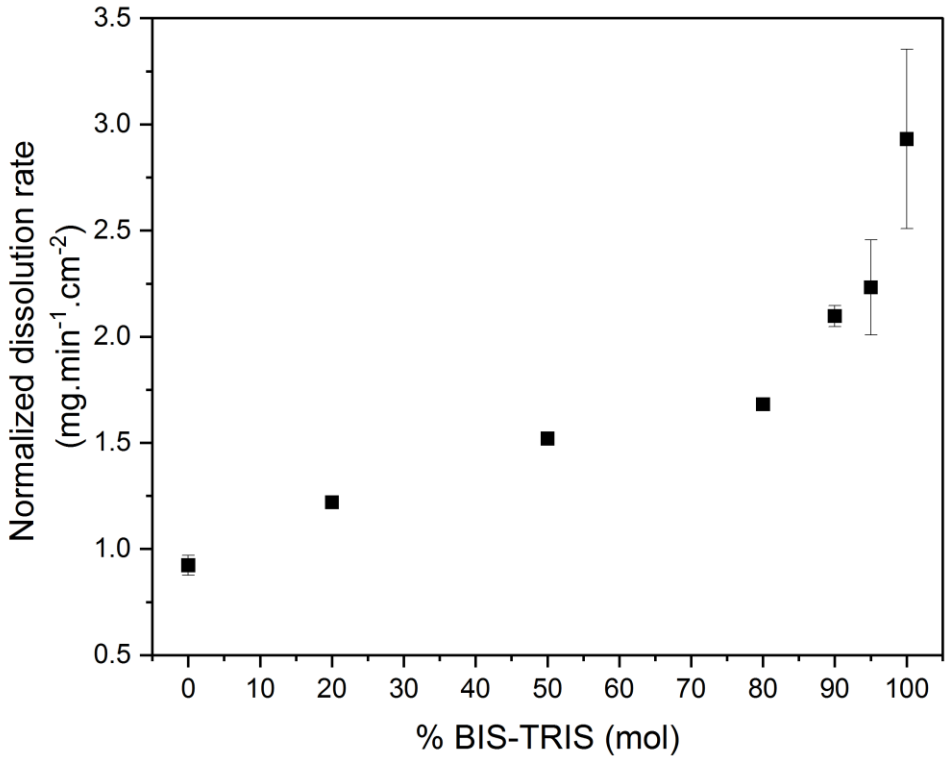

Figure 9. Normalized HP-50 release rate of HP-50-BIS-TRIS at different ionization extent. Error bars indicate standard deviation, n = 3.

4.9. Release Profiles of Miconazole-HP-50-X (X = H, Na, TEA) ASDs

Given that the ionized polymers show a faster release rate than the protonated polymer, the obvious next step was proof-of-concept studies with ASDs formulated with a lipophilic drug and a polymer salt. The impact of polymer salts with two different cations on the release behavior of miconazole, a representative BCS class II poorly soluble lipophilic drug with a p*K*a of 6.5,[15] was therefore studied by surface normalized dissolution of ASD compacts at a 20% drug loading. Figure 10 shows that release from HP-50 ASD was slow and incomplete, where the polymer released faster than the drug (incongruent release of components). Only 10% of the drug dose was released after 120 min. In contrast, the HP-50-Na ASD dissolved very quickly and exceeded the drug amorphous solubility (~5 µg/mL)[15] with the formation of a drug-rich phase leading to a turbid dissolution medium. Close to 90% drug release was observed after 60 min, whereby the polymer released at the same normalized rate as the drug. The drug release rate from the HP-50-Na ASD is 14 times faster than the drug release from the HP-50 ASD (Figure 11). A similar outcome was observed for the HP-50-TEA (PTEA) ASD (Figure 10, 11).

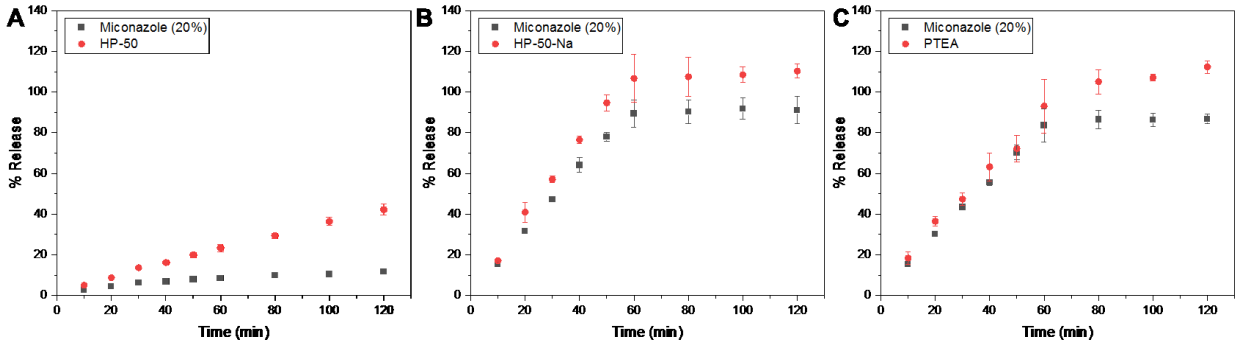

Figure 10: Impact of polymer salt versus protonated polymer on drug release for 20% drug loading ASDs. Error bars indicate standard deviation, n = 3.

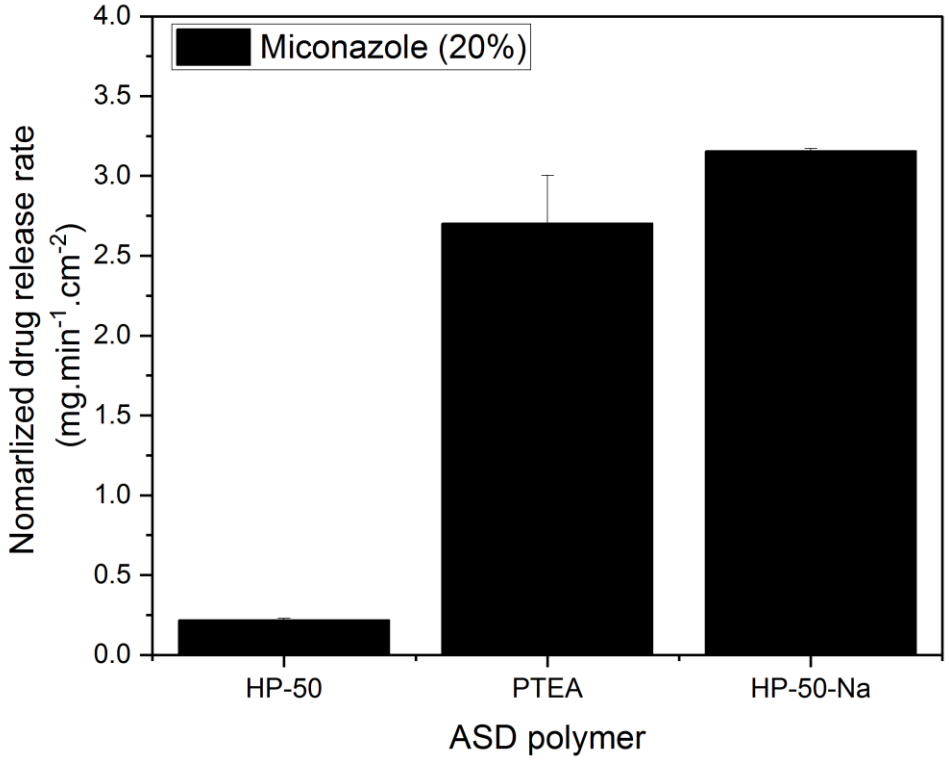

Figure 11: Normalized drug release rate of 20% drug loading ASDs comparing the protonated polymer with two polymer salts. Error bars indicate standard deviation, n = 3.

5. Discussion

Factors Impacting Polymer Dissolution Rate

It is well established that the dissolution rates of enteric polymers such as HPMCP are highly sensitive to the solution pH. The dissolution pH used in this study was 6.8 where HPMCP is

extensively ionized given a reported pK_a value of 4.2 and hence soluble.[20, 21] However, this is the bulk solution pH, and not the pH at the dissolving surface which may differ depending on the experimental conditions employed. The pH profile across the aqueous boundary layer has been the subject of several experimental and modeling studies. Thus, for dissolution of acidic molecules in media above the compound pK_a, the pH at the dissolving surface-water interface is typically lower than that of the bulk pH.[22-25] This phenomenon occurs due to the ionization of acidic molecules upon entering solution, resulting in liberation of protons, decreasing the pH at the interface. This in turn can reduce the compound solubility and dissolution rate if the surface pH is close to the compound pK_a. Protons liberated via ionization leave the interface by three mechanisms: Diffusion of the proton across the boundary layer into the bulk solution, diffusion of hydroxyl ions from the bulk solution to the interface followed by neutralization of the proton, or, in solutions containing buffer components, reaction with a proton carrier followed by diffusion of the protonated carrier from the interface to the bulk solution with subsequent release of the proton. While ionization reactions are considered instantaneous, a finite time is required for the diffusion of the protons, hydroxyl ions and proton carriers across the boundary layer that exists at the solid surface. Consequently a pH gradient from the surface (lower pH) to the bulk pH (higher pH) may be generated. Hydrodynamic conditions, solute pK_a and solubility as well as the properties of the buffer species (pK_a and concentration) impact the pH gradient across the boundary layer.[23] pH gradients have been demonstrated for both small molecules and enteric polymers.[5, 22-26] Of relevance to this study, a pH gradient has been previously reported for HP-50 films in phosphate buffer of similar buffer capacity to that used in this study.[5]

For small molecules, mass transfer across the boundary layer is the rate limiting step for dissolution. However, the situation is more complex for polymers. There are additional important processes involved in polymer dissolution that may be rate-limiting.[11, 27] For an acidic polymer that requires ionization for solubilization, these steps are: 1) ingress of water and hydroxyl ions into the glassy polymer, resulting in plasticization, an increase in polymer chain mobility and the formation of a gel layer, 2) polymer ionization, 3) polymer chain disentanglement, 4) further ionization of disentangled polymer chains at the polymer-solvent interface, 5) diffusion of the released polymer chains across the boundary layer and into the bulk solution.[11] For neutral water soluble polymers above the critical entanglement molecular weight, ingress of water or

polymer chain disentanglement are typically considered the rate limiting steps, rather than diffusion of polymer chains across the boundary layer. However, for polymers that dissolve by ionization, a different rate limiting step may dominante. In a study of Eudragit methacrylate/methacrylic acid polymer dissolution in different media, Nguyen and Fogler suggested that polymer dissolution can be either mass transport or chain disentanglement limited depending on hydrodynamic conditions and the concentration of proton-carrying buffer species.[11] They showed that for the mass transport limited regimen, the determining factor that impacted the polymer diffusion rate is the concentration of hydrogen ions at the polymer-solvent interface. When the H^+ concentration is high, polymer solubility is low, and hence the polymer diffusive flux into the bulk solution is low. Consequently, any factors that impact the interface H^+ concentration will affect the polymer dissolution rate. These factors include the bulk proton concentration, the polymer solubility, as well as the concentration of proton carriers and the affinity of the carrier and polymer for the protons (as determined by the pK_a values).

In the current study, proton carriers, in the form of buffer species, are present in all dissolution media, where the bulk pH was 6.8, more that 2 pH units above the pK_a (~4.2) of HP-50.[21] The polymer has high solubility at the bulk solution pH. However, even though all media had equivalent pH, differences were observed in the polymer intrinsic dissolution rate (Figure 2) highlighting the importance of the buffer properties. To remove protons from the polymer-water interface, the proton carrier needs to be able to accept a proton in the lower pH environment of the interface, diffuse to the bulk solution, and release the proton to regenerate the conjugate base. Therefore, the pK_a of the carrier relative to both the bulk pH and surface pH is important, and will impact the efficiency of the carrier, together with the proton carrier concentration. From Figure 2, the impact of the various buffers on polymer dissolution rate can be largely rationalized based on their pK_a values relative to the bulk solution pH. As can be seen from Figure 2, the dissolution rate follows the order BIS-TRIS>phosphate>tris>TEA. BIS-TRIS and phosphate have pK_a's close to the bulk solution pH (6.5 and 7.2 respectively, Table 1), and hence will have good proton binding and releasing capacity at the lower surface pH and the higher bulk pH respectively. Due to the lower pK_a, BIS-TRIS will have a higher concentration of the conjugate base at the surface pH (assuming a surface pH ~0.4 units lower than the bulk pH, as reported in other studies)[5] than phosphate, and thus will be more effective at conveying protons liberated from polymer ionization

into the bulk solution. In contrast, tris and TEA have higher pK_a's of 8.1, and 10.2 respectively (Table 1) and will exist predominantly as the conjugate acid (i.e. in protonated form) at surface and bulk pH conditions, and therefore cannot act as proton carriers, leading to slower polymer dissolution rates.

It is also of interest to consider if the properties of the cationic counterion, required for charge neutralization of the ionized polymer carboxylate group, plays a role. Previous studies have shown trends between counterion size and polymer dissolution rate.[18] Reiser used this observation in partial support of a percolation model for dissolution of an ionizing acidic polymer.[13] The basis for the percolation model is that diffusion of solvent species through the polymer gel, from one polymer ionizing site to the next, is the rate limiting step for dissolution. Arcus also found that the polymer dissolution rate decreased in a non-linear fashion with an increase in the specific volume of the base cation, presumably due to their slower diffusion rates. [18] The lack of correlation observed herein between counterion size and polymer dissolution rate (Figure 6) indicates that a percolation model of dissolution is likely not appropriate for HP-50. Instead, Nguyen and Fogler's observations that one of the important factors for acidic polymer dissolution is the polymer solubility at the interface, which in turn depends on the surface pH, and thus the buffer speciation in terms of the proton carrier concentration, appear to provide a better explanation for our observations.[11] Furthermore, the extent of hydration of the polymeric gel layer will also be affected by the surface pH, with less hydration occurring for a lower degree of polymer ionization. In turn, the solvent fraction in the gel layer will determine the polymer disentanglement rate.[28]

By elucidating that the rate limiting step for HP-50 dissolution is likely polymer solubilization and hydration via ionization, which is linked to the mass transport rate of protons and other key ionic species across the boundary layer, polymers can be designed with the goal of enhancing the dissolution rate. Results summarized in Figure 8 demonstrate that this goal is readily achieved by "pre-ionization" of the polymer through salt formation, eliminating the problematic generation and transport of protons. The polymer salt with the "simplest" counterion is the sodium salt. Direct comparison of HP-50 and HPMCP-Na dissolution under different conditions confirms the postulated roles of proton generation and removal rate via proton carriers as processes that hinder dissolution in the protonated polymer. First, in a widely used buffer system, 50 mM phosphate

buffer, HP-50-Na dissolves more than twice as fast as the protonated polymer. Second, the dissolution rate of HP-50-Na is not impacted by the buffer capacity (concentration of proton carriers), in contrast to that of HP-50. The latter polymer shows a 6-fold decrease in dissolution rate on decreasing the buffer capacity from 29 to 3 mM L^{-1} ΔpH^{-1} (phosphate buffer concentration decrease from 50 to 5 mM), while HP-50-Na maintains a rapid and equivalent dissolution rate under both conditions. Third, HP-50-Na dissolves in water (NMR spectrum shown in Figure S2-3), while HP-50 is insoluble (no NMR peaks observed following addition of polymer to water). Clearly, salt formation overcomes the dependence of polymer dissolution on the proton carrier concentration in the medium. This is an important observation as the proton carrier concentration is related to the buffer capacity of the dissolution medium, which shows both intra- and inter-individual variability *in vivo* and is much lower than for the commonly used *in vitro* dissolution test medium, 50 mM phosphate buffer.[29-34] Therefore, using a polymer salt for an ASD formulation may offer advantages in terms of both dissolution rate as well as robustness of the dissolution rate to local media conditions encountered in the intestine. Interestingly, the counterion used to make the polymer salt does not appear to impact the subsequent neat polymer dissolution rate (Figure 6). Thus, the pK_a of the base used to form the salt does not correlate with the dissolution rate, different from dissolution of the protonated polymer in a buffer solution prepared from the corresponding base. This is very apparent by comparing the dissolution rates of HP-50-TEA salt and HP-50 in TEA buffer (Figure S8). The observation that the counterion does not noticably impact the polymer salt dissolution rate is somewhat surprising given the water sorption data shown in Figure 7, where the water content is higher for the Na salt relative to the three ammonium salts evaluated. However, the four salts evaluated have a much higher tendency to absorb water than the protonated polymer, which will facilitate water ingress, the solvent volume fraction in the gel layer, and consequently, the rate of polymer chain disentanglement.[28] The improved hydration extent accompanying salt formation is likely a key contributor to the faster dissolution of the polymer salts.

The importance of the polymer existing in ionized form is also confirmed by the studies on the BIS-TRIS polymer salts with different extents of neutralization, where a decrease in ionization extent from 100 to 80% leads to an almost 2-fold decrease in dissolution rate. This observation is perhaps explained by considering that hydrophobic, water insoluble ionizable polymers require a

minimum extent of ionization to solubilize and commence dissolution.[35] Recently, Hiew and Taylor estimated that the critical ionization percent for HP-50 was approximately 83% ionization.[9] This may explain the notable impact of decreasing the ionization extent from 100 to 80% on the polymer dissolution rate. Of course, the partially ionized polymers are able to undergo further ionization upon contact with the dissolution medium, but are still impacted by the need for proton removal across the aqueous boundary layer, *albeit* to a lesser extent than the fully protonated polymer.

Historically, polymer neutralization has been explored for enteric coatings to enable development of non-latex based aqueous coating formulations.[36-38] More recently, partial polymer neutralization and a double coating strategy has been suggested as an approach to improve the dissolution of enteric coatings and reduce the lag time for release often observed following gastric emptying.[39] These efforts have focused on methacrylic acid/methacrylate polymers. However, the application of polymer salt formation as a strategy to improve ASD dissolution is an under-explored area. A prevailing issue with ASDs is the impact of the drug presence on the overall release performance. In other words, many ASDs show rapid release at low drug loadings, but the presence of a lipophilic drug causes a decline in release performance as the drug loading increases.[15, 40] This is exemplified by the 20% DL miconazole-HP-50 ASD shown in Figure 10, where only ~10% of the drug dose is released in an hour. In contrast, ASDs prepared with two of the polymer salts show complete drug release over the same time period. Given that low potency drugs are difficult to formulate as ASDs due to the high excipient burden, these initial studies highlight the potential advantage of polymer salts to enable higher drug loadings in ASD formulations without compromised release. It is likely that the higher hydration extent of the polymer salts relative to the protonated polymer helps to mitigate the deleterious impact of a lipophilic drug on the water solvent fraction in the gel layer, which is crucial to enable polymer chain disentanglement and release from the matrix. Although both polymer salts provide good release of miconazole at a 20% DL, it can be anticipated that at higher drug loadings, variations in the extent of hydration of different salts may play a role in dictating when the release performance deteriorates, and this will be evaluated in a future study.

Conclusions

Polymer salts of HP-50, synthesized with a variety of counterions, showed improved dissolution both as neat polymer salts, and when formulated as an amorphous solid disperion with miconazole, when compared to the protonated polymer. The improved dissolution rate of the ionized polymers, and consequently the enhanced drug release rate, is attributed to several factors. First, the polymer salt is "pre-ionized", and hence will undergo a higher extent and rate of hydration, leading to a more mobile gel layer, and enhanced release of polymer chains from the matrix. Second, no protons are generated at the solid-water interface, avoiding polymer solubility suppression resulting from the lowered surface pH. Additionally, polymer salt formation renders the dissolution process more robust to variations in media composition, in particular buffer capacity. Finally, when a lipophilic drug is incorporated into the polymer to form an amorphous solid dispersion, polymer salt formulations yield more extensive drug release than the corresponding protonated polymer ASD. This provides a potential formulation strategy to address a pressing concern with ASD formulations, notably the need to increase drug loading without compromising release performance. Given the wide array of counterions available to make pharmaceutically acceptable polymer salts, this strategy offers a relatively unexplored approach to modify polymer properties to potentially improve and expand the ASD formulation and processing space.

Acknowledgements

We thank the National Science Foundation (PFI-RP) for partial support of this work through grant IIP-1827493. Dana Moseson is thanked for assistance with TGA measurements. Alexandru Deac is acknowledged for help with FTIR spectroscopy experiments and Hanh Thuy Nguyen for assistance with statistical analysis. Alex Avdeef is thanked for performing buffer capacity measurements.

Supplemental information

The Supporting Information is available free of charge at

NMR spectra of synthesized new polymers, HP-50-X structures, radii of the cations, buffer composition, effect of buffer species on the dissolution of neat HP-50, TGA and FTIR profiles of HP-50-Na, t-test for the release profiles of HP-50-X

References

[1] D. Catteau, C. Barthelemy, M. Deveaux, H. Robert, F. Trublin, X. Marchandise, H. Van Drunen, Contribution of scintigraphy to verify the reliability of different preparation processes for enteric coated capsules, European journal of drug metabolism and pharmacokinetics, 19 (1994) 91-98.

[2] K. Lehmann, B. Broegmann, C. Kenyon, I. Wilding, The in vivo behaviour of enteric naproxen tablets coated with an aqueous dispersion of methacrylic acid copolymer, STP pharma sciences, 7 (1997) 463-468.

[3] I.R. Wilding, J.G. Hardy, R.A. Sparrow, S.S. Davis, P.B. Daly, J.R. English, In vivo evaluation of enteric-coated naproxen tablets using gamma scintigraphy, Pharmaceutical research, 9 (1992) 1436-1441.

[4] S.S. Ozturk, B.O. Palsson, B. Donohoe, J.B. Dressman, Kinetics of release from enteric-coated tablets, Pharmaceutical research, 5 (1988) 550-565.

[5] A.I. Harianawala, R.H. Bogner, M. Bradley, Measurement of pH near dissolving enteric coatings, International journal of pharmaceutics, 247 (2002) 139-146.

[6] S.V. Bhujbal, B. Mitra, U. Jain, Y. Gong, A. Agrawal, S. Karki, L. Taylor, S. Kumar, Q. Zhou, Pharmaceutical amorphous solid dispersion: A review of manufacturing strategies, Acta Pharmaceutica Sinica B, (2021) 2506-2537.

[7] D.M. Mudie, A.M. Stewart, J.A. Rosales, N. Biswas, M.S. Adam, A. Smith, C.D. Craig, M.M. Morgen, D.T. Vodak, Amorphous Solid Dispersion Tablets Overcome Acalabrutinib pH Effect in Dogs, Pharmaceutics, 13 (2021) 557.

[8] A. Elkhabaz, S. Sarkar, G.J. Simpson, L.S. Taylor, Characterization of phase transformations for amorphous solid dispersions of a weakly basic drug upon dissolution in biorelevant media, Pharmaceutical research, 36 (2019) 1-17.

[9] T.N. Hiew, D.Y. Zemlyanov, L.S. Taylor, Balancing solid-state stability and dissolution performance of lumefantrine amorphous solid dispersions: the role of polymer choice and drug–polymer interactions, Molecular Pharmaceutics, 19 (2022) 392-413.

[10] B. Hunek, E. Cussler, Mechanisms of photoresist dissolution, AIChE journal, 48 (2002) 661-672.

[11] D.A. Nguyen, H.S. Fogler, Facilitated diffusion in the dissolution of carboxylic polymers, AIChE journal, 51 (2005) 415-425.

[12] P.C. Tsiartas, L.W. Flanagin, C.L. Henderson, W.D. Hinsberg, I.C. Sanchez, R.T. Bonnecaze, C.G. Willson, The mechanism of phenolic polymer dissolution: A new perspective, Macromolecules, 30 (1997) 4656-4664.
[13] T.F. Yeh, H.Y. Shih, A. Reiser, Percolation view of novolak dissolution and dissolution inhibition, Macromolecules, 25 (1992) 5345-5352.
[14] S. Saboo, D.E. Moseson, U.S. Kestur, L.S. Taylor, Patterns of drug release as a function of drug loading from amorphous solid dispersions: A comparison of five different polymers, European Journal of Pharmaceutical Sciences, 155 (2020) 105514.
[15] R. Yang, A.K. Mann, T. Van Duong, J.D. Ormes, G.A. Okoh, A. Hermans, L.S. Taylor, Drug Release and Nanodroplet Formation from Amorphous Solid Dispersions: Insight into the Roles of Drug Physicochemical Properties and Polymer Selection, Molecular Pharmaceutics, 18 (2021) 2066-2081.
[16] J. Mangas-Sánchez, E. Busto, V. Gotor-Fernández, F. Malpartida, V. Gotor, Asymmetric chemoenzymatic synthesis of miconazole and econazole enantiomers. The importance of chirality in their biological evaluation, The Journal of organic chemistry, 76 (2011) 2115-2122.
[17] N. Li, J.D. Ormes, L.S. Taylor, Leaching of lopinavir amorphous solid dispersions in acidic media, Pharmaceutical research, 33 (2016) 1723-1735.
[18] R. Arcus, A membrane model for positive photoresist development, in: Advances in Resist Technology and Processing III, International Society for Optics and Photonics, 1986, 124-134.
[19] E. Shek, Buffer capacity, not buffer catalysis, affects the dissolution rate of cellulose acetate phthalate, Pharmaceutical Industry, 40 (1978) 981-982.
[20] J. Spitael, R. Kinget, Solubility and dissolution rate of enteric polymers, Acta Pharm Technol, 25 (1979) 163-168.
[21] M. Davis, I. Ichikawa, E. Williams, G. Banker, Comparison and evaluation of enteric polymer properties in aqueous solutions, International journal of pharmaceutics, 28 (1986) 157-166.
[22] K. Mooney, M. Mintun, K. Himmelstein, V. Stella, Dissolution kinetics of carboxylic acids I: effect of pH under unbuffered conditions, Journal of pharmaceutical sciences, 70 (1981) 13-22.
[23] K. Mooney, M. Mintun, K. Himmelstein, V. Stella, Dissolution kinetics of carboxylic acids II: Effect of buffers, Journal of pharmaceutical sciences, 70 (1981) 22-32.

[24] W. Higuchi, E.L. Parrott, D.E. Wurster, T. Higuchi, Investigation of drug release from solids II. Theoretical and experimental study of influences of bases and buffers on rates of dissolution of acidic solids, Journal of the American Pharmaceutical Association, 47 (1958) 376-383.
[25] B. Hens, N. Seegobin, M. Bermejo, Y. Tsume, N. Clear, M. McAllister, G.E. Amidon, G.L. Amidon, Dissolution Challenges Associated with the Surface pH of Drug Particles: Integration into Mechanistic Oral Absorption Modeling, The AAPS Journal, 24 (2022) 1-11.
[26] S.S. Ozturk, B.O. Palsson, J.B. Dressman, Dissolution of Ionizable Drugs in Buffered and Unbuffered Solutions, Pharmaceutical research, 5 (1988) 272-282.
[27] B.A. Miller-Chou, J.L. Koenig, A review of polymer dissolution, Progress in Polymer Science, 28 (2003) 1223-1270.
[28] B. Narasimhan, N.A. Peppas, Disentanglement and reptation during dissolution of rubbery polymers, Journal of Polymer Science Part B: Polymer Physics, 34 (1996) 947-961.
[29] Z. Vinarov, M. Abdallah, J.A. Agundez, K. Allegaert, A.W. Basit, M. Braeckmans, J. Ceulemans, M. Corsetti, B.T. Griffin, M. Grimm, Impact of gastrointestinal tract variability on oral drug absorption and pharmacokinetics: An UNGAP review, European Journal of Pharmaceutical Sciences, 162 (2021) 105812.
[30] B. Hens, Y. Tsume, M. Bermejo, P. Paixao, M.J. Koenigsknecht, J.R. Baker, W.L. Hasler, R. Lionberger, J. Fan, J. Dickens, Low buffer capacity and alternating motility along the human gastrointestinal tract: implications for in vivo dissolution and absorption of ionizable drugs, Molecular pharmaceutics, 14 (2017) 4281-4294.
[31] L. Kalantzi, K. Goumas, V. Kalioras, B. Abrahamsson, J.B. Dressman, C. Reppas, Characterization of the human upper gastrointestinal contents under conditions simulating bioavailability/bioequivalence studies, Pharmaceutical research, 23 (2006) 165-176.
[32] E. Jantratid, N. Janssen, C. Reppas, J.B. Dressman, Dissolution media simulating conditions in the proximal human gastrointestinal tract: an update, Pharmaceutical research, 25 (2008) 1663-1676.
[33] E.M. Persson, A.-S. Gustafsson, A.S. Carlsson, R.G. Nilsson, L. Knutson, P. Forsell, G. Hanisch, H. Lennernäs, B. Abrahamsson, The effects of food on the dissolution of poorly soluble drugs in human and in model small intestinal fluids, Pharmaceutical research, 22 (2005) 2141-2151.

[34] C.A. Bergström, R. Holm, S.A. Jørgensen, S.B. Andersson, P. Artursson, S. Beato, A. Borde, K. Box, M. Brewster, J. Dressman, Early pharmaceutical profiling to predict oral drug absorption: current status and unmet needs, European Journal of Pharmaceutical Sciences, 57 (2014) 173-199.
[35] J. Heller, R. Baker, R. Gale, J. Rodin, Controlled drug release by polymer dissolution. I. Partial esters of maleic anhydride copolymers—properties and theory, Journal of Applied Polymer Science, 22 (1978) 1991-2009.
[36] S.R. Béchard, L. Levy, S.-D. Clas, Thermal, mechanical and functional properties of cellulose acetate phthalate (CAP) coatings obtained from neutralized aqueous solutions, International Journal of Pharmaceutics, 114 (1995) 205-213.
[37] J. Stafford, S. Ag, Enteric film coating using completely aqueous dissolved hydroxypropyl methyl cellulose phthalate spray solutions, Drug Development and Industrial Pharmacy, 8 (1982) 513-530.
[38] R.-K. Chang, A comparison of rheological and enteric properties among organic solutions, ammonium salt aqueous solutions, and latex systems of some enteric polymers, Pharm Technol, 14 (1990) 62-70.
[39] F. Liu, R. Lizio, C. Meier, H.-U. Petereit, P. Blakey, A.W. Basit, A novel concept in enteric coating: a double-coating system providing rapid drug release in the proximal small intestine, Journal of Controlled Release, 133 (2009) 119-124.
[40] A.S. Indulkar, X. Lou, G.G. Zhang, L.S. Taylor, Insights into the dissolution mechanism of ritonavir–copovidone amorphous solid dispersions: Importance of congruent release for enhanced performance, Molecular pharmaceutics, 16 (2019) 1327-1339.